Available online at www.sciencedirect.com
SCIENCE DIRECT
Journal of Catalysis 239 (2006) 290–298
JOURNAL OF CATALYSIS
www.elsevier.com/locate/jcat

Microwave frequency effects on synthesis of cryptomelane-type manganese oxide and catalytic activity of cryptomelane precursor

Kinga A. Malinger [a], Yun-Shuang Ding [b], Shanthakumar Sithambaram [a], Laura Espinal [b], Sinue Gomez [b], Steven L. Suib [a,b,*]

[a] *Chemistry Department, University of Connecticut, 55 N. Eagleville road, Storrs, CT 06269-3060, USA*
[b] *Institute of Materials Science, University of Connecticut, 55 N. Eagleville road, Storrs, CT 06269-3060, USA*

Received 18 November 2005; revised 31 January 2006; accepted 8 February 2006

Available online 10 March 2006

Abstract

Cryptomelane-type manganese oxides (OMS-2) were synthesized in the presence of microwave heating at different microwave frequencies and also using variable-frequency heating. The materials were prepared using a two-step hydrothermal procedure. Catalytic activity of the materials was tested for the oxidation of 2-thiophenemethanol. OMS-2 prepared at a high-frequency limit of 5.5 GHz showed the highest conversion (50%) to the 2-thiophenecarboxaldehyde among all of the tested OMS-2 samples. The OMS-2 precursor showed remarkable conversion (89%) in the oxidation reaction. In addition, the OMS-2 materials and the precursor showed differences in oxygen evolution based on the thermal decomposition experiments, as well as differences in porosity.

Keywords: Cryptomelane; Microwave heating; Microwave frequency; Catalytic oxidation

1. Introduction

Cryptomelane (OMS-2) is a microporous tunnel-structured manganese oxide-type material. The mixed valency of manganese makes OMS-2 a good semiconductor and oxidation catalyst. Synthetic cryptomelane (OMS-2) is composed of MnO_6 octahedra that are edge- and corner-shared. K^+ is the predominant cation in the tunnel besides water molecules. The tunnel size is 4.6×4.6 Å because of the 2×2 arrangement of the MnO_6 octahedra. The average manganese oxidation state in OMS-2 is around 3.8, containing a mixture of Mn^{4+}, Mn^{3+}, and Mn^{2+} ions [1–3]. Preparation of cryptomelane-type manganese oxides is easy and inexpensive. Various synthetic routes have been explored, including reflux [4,5], thermal or hydrothermal treatment of birnessites [6,7], and a sol–gel route [8,9]. The reflux method, involving the oxidation of Mn^{2+} by $KMnO_4$, is the most common route for preparing bulk OMS-2 materials. These materials have shown good catalytic activity in alcohol oxidation [10,11].

The use of microwave radiation in chemistry has been extensively studied, and a number of publications have covered this topic. Virtually all reaction types have been tested in a microwave field. Many chemical reactions and processes can be accelerated [12–14], and in some cases selectivity can be improved [15–17]. The amount of coupling with the electric field of microwave radiation depends on the material type, namely, the dielectric constant. The dielectric constant characterizes the ability of the material to be polarized by the electric field [18]. Rapid heating occurs due to interaction of microwaves with either dipolar molecules or ionic species [19]. Some researchers believe that acceleration of microwave-assisted reaction rates might be due to a different mode of transferring heat to reagents and solvents. Others believe that absorption of microwave radiation has some specific activating (nonthermal) effect on microwave-absorbing molecules [20,21]. However, reasons for the so-called "nonthermal" effects, like the enhanced catalytic activity of the microwave-prepared materials, remain to be fully explored and understood. Regardless, microwave processing

* Corresponding author. Fax: +1 860 486 2981.
E-mail address: steven.suib@uconn.edu (S.L. Suib).

0021-9517/$ – see front matter
doi:10.1016/j.jcat.2006.02.005

provides an alternative and promising way of producing materials with improved properties according to reports in the literature [12,13,15].

Water is a very good medium for microwave-assisted synthesis due to its high dielectric constant. Energy created by solvent absorption leads to efficient heating of the reaction mixture [22,23]. Manganese oxides have also been reported to have a very high dielectric constant of ∼10,000; therefore, good coupling can be expected with microwave radiation [24–26]. Microwave heating may produce some interesting effects as compared with conventional heating.

There is a significant difference between variable-frequency microwave (VFMW) heating and regular microwave heating. During a VFMW operation, a selected bandwidth is swept around a central frequency in a specified time, which keeps the microwave energy from remaining focused at any given location for more than a fraction of a second. Therefore, VFMW frequency processes result in time-averaged heating [27,28]. In the presence of standing waves of electric fields during constant frequency microwave operation, arcing occurs from a charge build-up in conductive materials. Arcing problems and localized heating are eliminated using VFMW techniques [29]. Application of different microwave frequencies and a VFMW operation during the synthesis process could affect the properties of materials.

2. Experimental

2.1. Synthesis

A two-step procedure was applied to prepare OMS-2 materials. First, the OMS-2 precursor was prepared by a precipitation reaction. Manganese acetate water solution was added dropwise to a solution of potassium permanganate under vigorous stirring at room temperature. The resultant brownish precipitate was stirred for 24 h, followed by thorough washing with distilled deionized water. The precursor was placed in its wet form in Teflon autoclaves, sealed, and hydrothermally treated in a convection oven and a microwave furnace at 100 °C. The same amount of the precursor was used for all syntheses, and approximately the same volumes were used for the conventional and microwave syntheses. The synthesis with conventional heating took up to 24 h, whereas microwave-assisted synthesis took 4 h. Approximately 0.5 g of each OMS-2 material was obtained. Microwave frequencies of 2.45 GHz, 5.5 GHz, and variable-frequency programs were used for the hydrothermal treatment step. During the variable-frequency program, the microwave frequency was swept continuously in the 3–5.5 GHz range with a sweeping time of 1 s. The microwave power was generated at approximately 100 W during the synthesis. The materials were washed and calcined at 120 °C.

2.2. Characterization

2.2.1. X-Ray powder diffraction

The X-ray powder diffraction patterns of the samples were collected using a Scintag 2000 PDS instrument with Cu-K_α X-ray radiation with a 1.5418 Å wavelength. A beam voltage of 45 kV and a 40-mA beam current were used. The JCPDS database was used to identify the phases.

2.2.2. Field emission electron spectroscopy

The morphology was studied by field emission scanning electron microscopy (FESEM) on a Zeiss DSM 982 Gemini instrument with a Schottky emitter at an accelerating voltage of 2 kV and a beam current of about 1 μÅ. The samples were prepared for analyses by dispersing them in distilled deionized water. Droplets of the suspensions were placed on a gold-coated silicon wafer.

2.2.3. Transmission electron microscopy

Transmission electron microscopy (TEM) images were obtained with a JEOL 2010 FasTEM at an accelerating voltage of 200 kV. Powder samples were dispersed ultrasonically in 2-propanol, and the suspension was deposited on a Quantafoil holey carbon-coated copper grid (R1.2/1.3).

2.2.4. Specific surface area and porosity measurements

The nitrogen sorption measurements were performed using a Micrometrics ASAP 2010 accelerated surface area system. The adsorption and desorption experiments were done at 77 K after initial pretreatment of the samples by degassing at 130 °C for 12 h. The specific surface areas of the samples were determined by the BET method, and the micropore size distribution was reported using the Horvath–Kawazoe (HK) model. The mesopore/macropore size distribution was calculated by the BJH method using the desorption data.

2.2.5. Thermal stability

The thermal stability of the samples was studied by thermogravimetric analysis (TGA). The experiments were done with a TA Instrument model 2950 under N_2 atmosphere. The temperature was increased from 30 to 900 °C at a rate of 10 °C/min during the experiments.

2.2.6. Temperature-programmed decomposition

Analyses of outlet gases during thermal treatment of the OMS-2 samples were performed by temperature-programmed decomposition using mass spectrometry (TPD–MS). About 30 mg of each sample was loaded into a quartz tube, placed in a tubular furnace controlled with an Omega temperature controller, and purged with UHP He (Matheson) for 4 h at room temperature. The samples were subsequently heated to 700 °C at a rate of 15 °C/min in He. The exhaust carrier gas was collected with an MKS-UTI PPT quadrupole residual gas analyzer to monitor the evolution of water and oxygen.

2.2.7. Raman spectroscopy

Raman spectra were taken at room temperature in the range of 100–2000 cm^{-1} with a Renishaw 2000 Raman microscope setup, which includes an optical microscope and a CCD camera for multichannel detection. A 514-nm argon ion laser was used to record the spectra for the conventional OMS-2 and the precursor.

2.2.8. Average oxidation state determination

A potentiometric titration was used to measure the average oxidation state of manganese in all of the samples. This method comprises a two-step procedure, with the first step involving determination of the total manganese content in a sample and the second step measuring the amount of available oxygen in the sample. A complete titration procedure has been described previously [30].

2.3. Catalytic reactions

For the oxidation of 2-thiophenemethanol, 1 mmol of 2-thiophenemethanol and 10 mL of toluene were placed in a 50-mL round-bottomed flask. Conventionally or microwave synthesized OMS-2 (50 mg) was added to this mixture. The OMS-2 precursor was also tested for catalytic activity. The reaction mixtures were stirred and refluxed at 110 °C for 4 h under an air atmosphere, then filtered. The recovered precursor catalyst was washed with methanol, calcined at 250 °C, and tested for reusability. The products of the experiment were analyzed and quantified by GC-MS.

2.3.1. Product analysis

Identification and quantification of the reaction products were done by GC-MS using an HP 5890 Series II gas chromatograph coupled with an HP 5971 mass detector for the product analyses. An HP-1 (nonpolar cross-linked siloxane) column with dimensions of 12.5 m × 0.2 mm × 0.33 μm was used.

3. Results

3.1. Structure and morphology

The XRD results of the prepared materials are illustrated in Fig. 1. The patterns are consistent with the Q-phase of cryptomelane (KMn_8O_{16}; JCPDS 29-1020). The OMS-2 precursor appears to be amorphous manganese oxide with little crystallinity and showing two broad peaks, one at $d = 2.389$ Å, which matches the strongest line for cryptomelane, and another at $d = 3.937$ Å. The JCPDS pattern of the Q-cryptomelane phase is shown at the bottom of the figure.

Fig. 2 shows FESEM micrographs of the prepared materials. All of the samples display fibrous morphologies typical of cryptomelane regardless of the type of hydrothermal treatment used. The fibers are a few hundred nm long and <100 nm in diameter. The OMS-2 precursor shows a chunky morphology. The cryptomelane samples obtained under different hydrothermal treatments do not show the presence of the precursor.

TEM micrographs show the details of the crystal structure of the materials. Fig. 3 illustrates the morphology of the OMS-2 precursor. The sample appears to be mainly amorphous, with some parts showing crystallinity. OMS-2 prepared at low microwave frequency (2.45 GHz) revealed cryptomelane morphologies, as shown in Fig. 4. The inset in Fig. 4a shows electron diffraction for a single fiber of the OMS-2 material prepared with microwaves at 2.45 GHz. The d-spacing values calculated from the diffraction pattern are in good agreement with the XRD data for Q-cryptomelane (KMn_8O_{16}; JCPDS 29-1020). Fig. 5 shows TEM analysis of OMS-2 prepared at high frequency (5.5 GHz). This sample reveals a nonuniform morphology consisting of cryptomelane-like fibers as well as smaller crystallites <100 nm long (Fig. 5b). The ratio of larger to smaller crystallites is approximately 1:1 based on the TEM images. The inset in Fig. 5a shows the electron diffraction for OMS-2 prepared with microwaves at 5.5 GHz. The ring pattern suggests that the crystallites are randomly oriented, and the d-spacings calculated from the ring pattern are consistent with the JCPDS file for Q-cryptomelane.

3.2. Surface area, porosity, and Mn average oxidation state

Table 1 presents the total pore volume, micropore volume, average pore diameter, and BET surface area of each OMS-2 material. All of the samples show similar N_2 adsorption/desorption isotherms typical of mesoporous materials. A representative type II isotherm for conventionally prepared

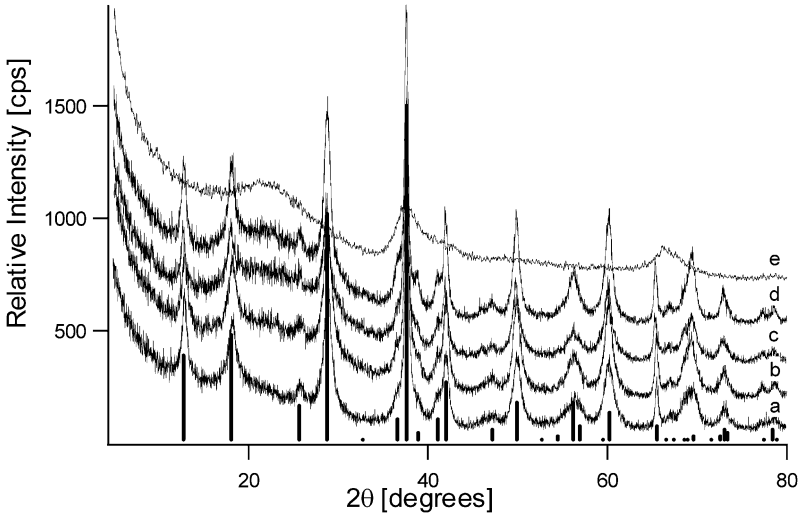

Fig. 1. X-Ray diffraction of OMS-2 made: (a) conventionally, (b) at 2.45 GHz, (c) at 5.5 GHz, (d) at variable frequency. XRD pattern for the precursor (e).

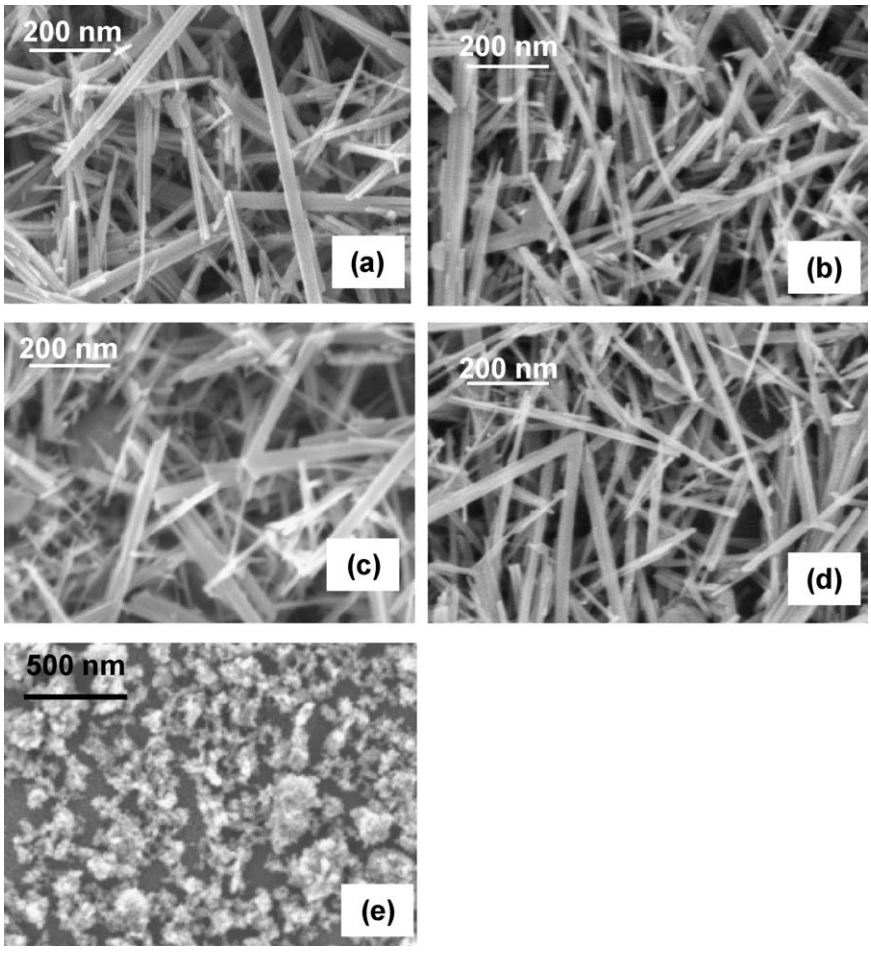

Fig. 2. FESEM images of OMS-2 made: (a) conventionally, (b) at 2.45 GHz, (c) at 5.5 GHz, (d) at variable frequency. Part (e) depicts the precursor morphology.

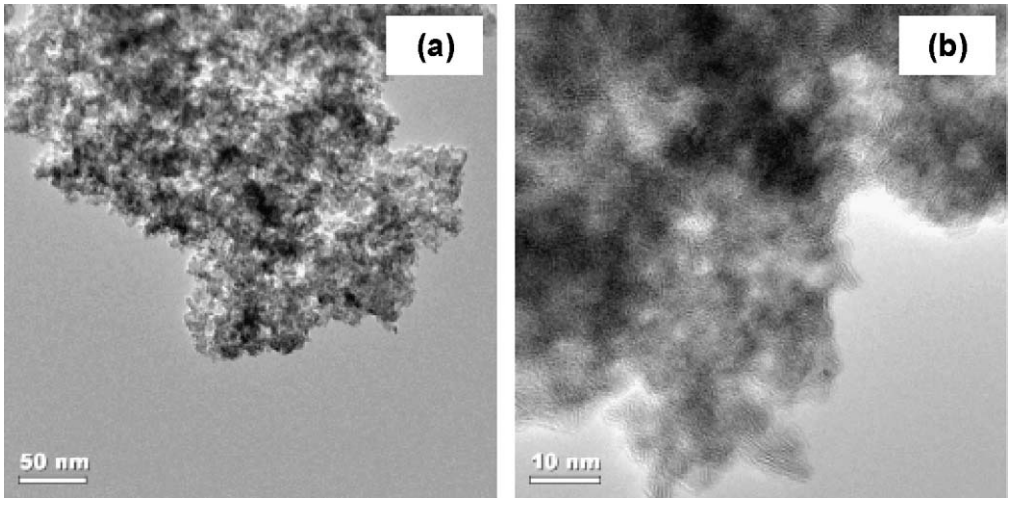

Fig. 3. TEM images of the OMS-2 precursor: (a) low magnification, (b) high magnification.

OMS-2 is shown in Fig. 6. The figure's inset shows the macropore size distribution calculated by the BJH method with a major pore size diameter of ∼530 Å. Fig. 7 depicts the isotherm and macropore size distribution plot for OMS-2 synthesized at 5.5 GHz. All of the cryptomelane samples show a very wide pore size distribution and BET surface areas in the same range. The OMS-2 precursor exhibits a relatively narrow pore size distribution, with an average pore diameter of 64 Å (Fig. 8). The BET surface area of the precursor is 273 m_2/g, around four times higher than that of OMS-2. The OMS-2 precursor shows a higher percentage of micropore volume (∼3.6%) than the OMS-2 samples. Fig. 9 shows an HK differential pore

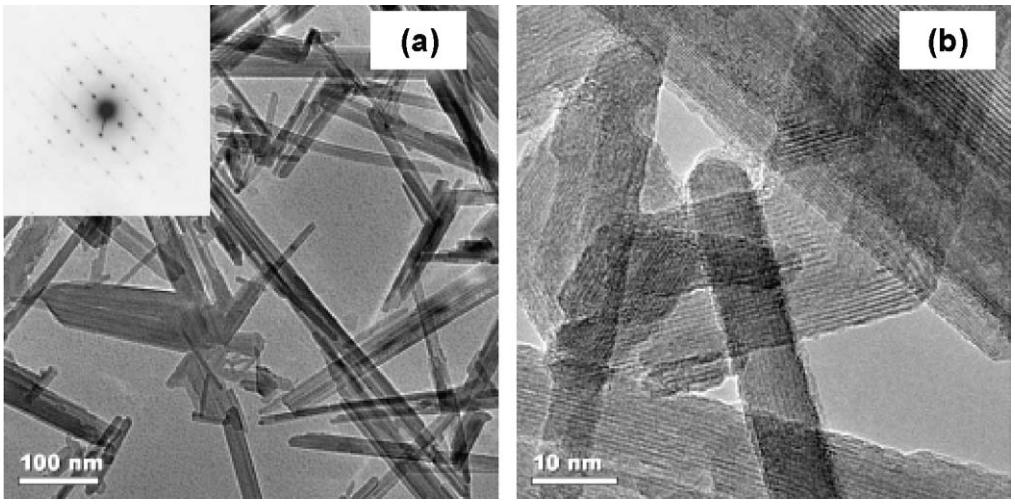

Fig. 4. TEM images of the low microwave frequency OMS-2: (a) low magnification (the insert shows electron diffraction pattern for the single fiber), (b) high magnification.

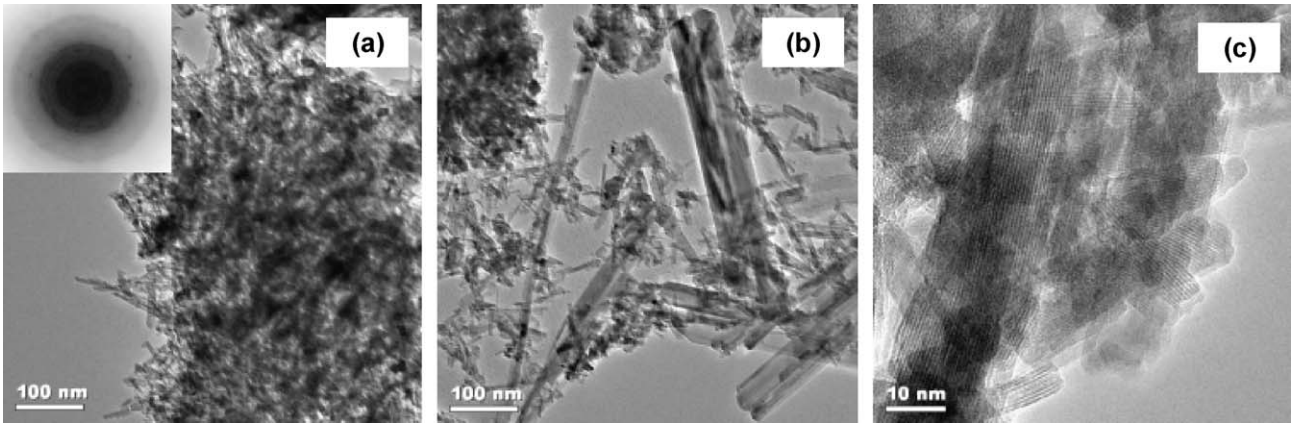

Fig. 5. TEM images of the high frequency OMS-2: (a) and (b) low magnification (the insert shows the electron diffraction pattern), (c) high magnification.

Table 1
N_2 physisorption and Mn average oxidation state (AOS) determination results for the OMS-2 samples

	Average pore diameter (Å)	Total pore volume (cm^3/g)	Micropore volume (cm^3/g)	BET surface area (m^2/g)	AOS ±0.2
Conventional OMS-2	151	0.272	0.0030	67	3.72
2.45 GHz OMS-2	245	0.489	0.0031	80	3.92
5.5 GHz OMS-2	189	0.307	0.0042	73	3.75
Variable frequency OMS-2	271	0.437	0.0061	65	4.02
OMS-2 Precursor	64	0.468	0.0170	273	3.79

volume plot for the OMS-2 precursor indicating an average micropore size of the precursor of 5.7 Å. High-frequency OMS-2 (5.5 GHz) also showed quite a high micropore content (∼2%) compared with the remaining OMS-2 samples.

Table 1 also contains results of the average oxidation state determination for manganese. Conventionally made OMS-2 appears to have the lowest AOS of manganese. The material prepared at variable-frequency operation revealed the highest Mn AOS. The AOSs for manganese for all of the prepared materials fall within a range characteristic for OMS-2.

3.3. Thermal stability

The results of TGA analyses are displayed in Fig. 10. All the OMS-2 samples synthesized under different types of heating show similar thermal behavior. Three major weight losses occur between 25 and 750 °C. The first weight loss, occurring at up to 450 °C, is about 3% and can be attributed to physisorbed and chemisorbed water. The second weight loss, ∼6%, occurring at 450–650 °C, is due to oxygen evolution from OMS-2 materials, as reported previously [31]. The third weight loss, of

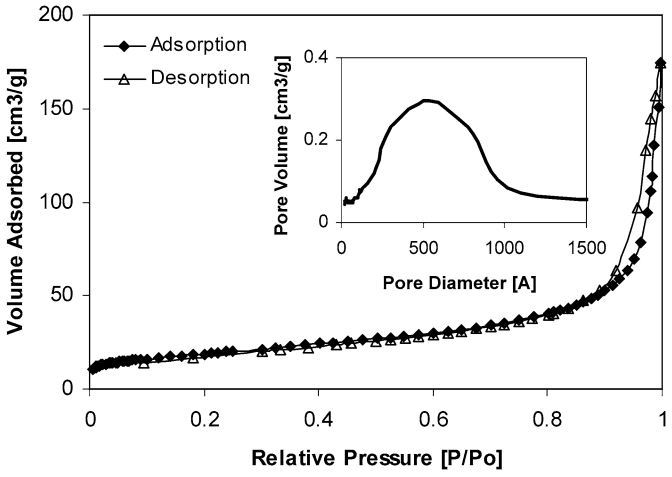

Fig. 6. N_2 adsorption/desorption isothermal plot of OMS-2 prepared by the conventional hydrothermal technique. The insert shows the pore size distribution plot by BJH method.

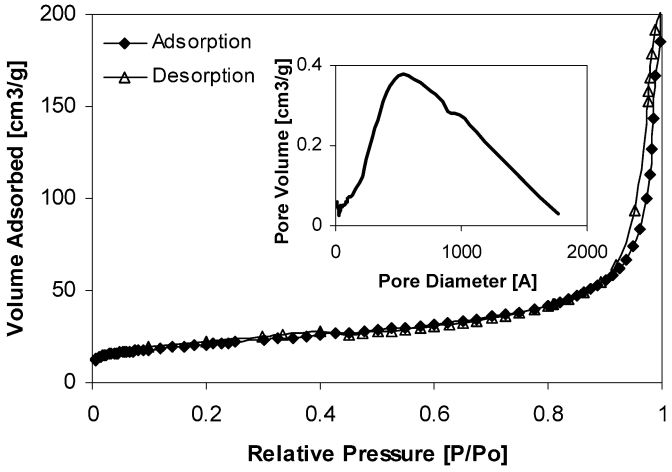

Fig. 7. N_2 adsorption/desorption isothermal plot of OMS-2 prepared at 5.5 GHz microwave frequency. The insert shows the pore size distribution plot by BJH method.

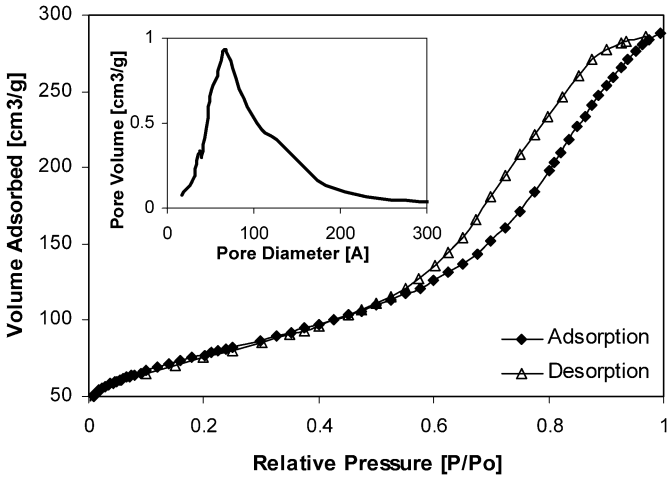

Fig. 8. N_2 adsorption/desorption isothermal plot of the OMS-2 precursor. The insert shows the mesopore size distribution plot by BJH method.

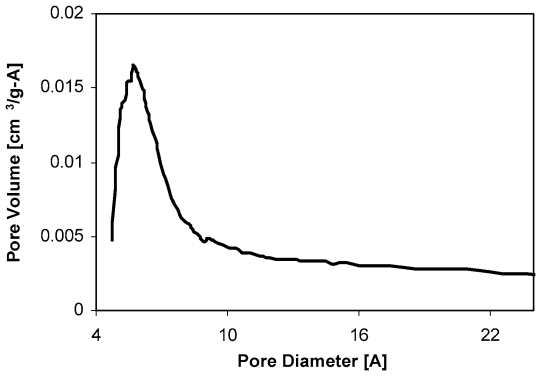

Fig. 9. Horvath–Kawazoe micropore-size distribution for the OMS-2 precursor.

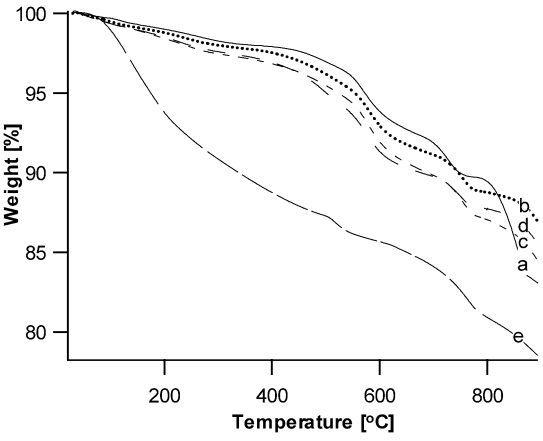

Fig. 10. Thermogravimetric analyses of OMS-2 made: (a) conventionally, (b) at 2.45 GHz, (c) at 5.5 GHz, (d) at variable frequency. TGA analysis of OMS-2 precursor (e).

approximately 3%, is due to the second lattice oxygen release at 650–750 °C. The materials decompose to hausmannite during the analyses.

3.4. Temperature-programmed decomposition

Fig. 11 illustrates the evolution of oxygen from the OMS-2 precursor and OMS-2 materials as a function of temperature. This oxygen peak appears as the lattice oxygen is liberated due to heating in a He atmosphere. The temperature at which the oxygen peak appears is the temperature at which the Mn–O bond is broken and represents the thermal stability limit for that material. The oxygen peaks can be classified as low-temperature (LT), medium-temperature (MT), and high-temperature (HT) peaks, based on their evolution temperature [32–34]. All of the materials show a major oxygen evolution peak between 500 and 560 °C. The second, smaller oxygen peak appears approximately 100 °C later. The O_2 profile for the OMS-2 precursor differs dramatically from those for the OMS-2 samples. Oxygen begins to evolve at 200 °C and appears as a broad bump in the TPD graph. It also gives a sharp maximum at 500 °C. The second oxygen peak emerges at 700 °C. Low- and variable-frequency cryptomelanes both start giving oxygen on heating at around 365 °C and show maxima at 500 °C. In contrast, high-frequency cryptomelane shows oxy-

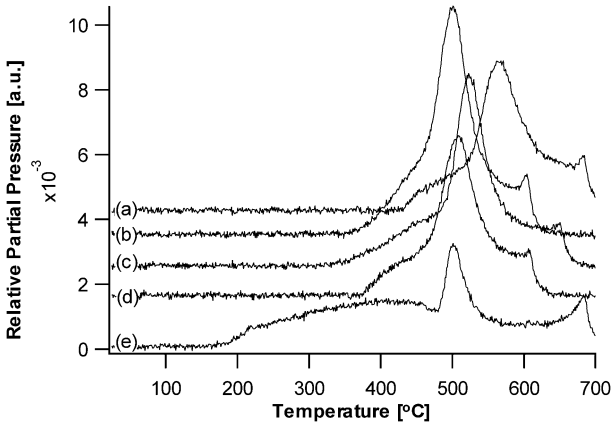

Fig. 11. Oxygen evolution during temperature-programmed decomposition of: (a) conventional OMS-2, (b) 2.45 GHz OMS-2, (c) 5.5 GHz OMS-2, (d) variable frequency OMS-2, (e) precursor.

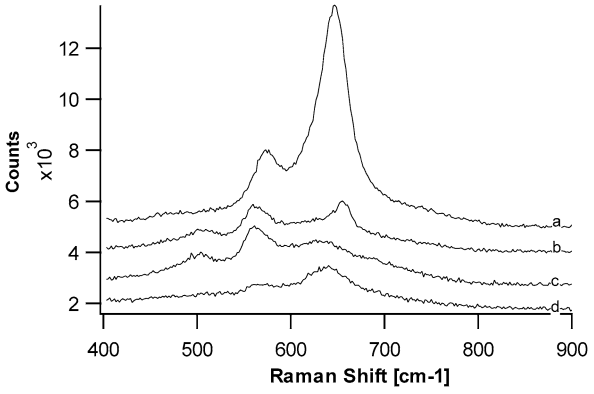

Fig. 12. Raman spectra of OMS-2 (a) and the precursor: (b), (c), and (d).

gen release as early as at 300 °C, with a slow increase to reach a maximum at 520 °C. Conventionally prepared OMS-2 begins to give off oxygen at a much higher temperature (∼430 °C) and shows a maximum at 565 °C.

3.5. Raman spectroscopy

Raman spectra of the conventional OMS-2 and the OMS-2 precursor are represented in Fig. 12. The cryptomelane sample shows a weak band at 570^{-1} and a much stronger band at 645 cm^{-1}. The precursor revealed different spectra for the different areas of the material. The sample contains a spectrum similar to that for cryptomelane, as well as spectra that may be associated with different types of manganese oxides. The precursor showed peaks at 500, 560, 635, and 655 cm^{-1}. Bands at 500–510, 575–580, and 630–640 cm^{-1} can be attributed to MnO_2. The peak at 650 cm^{-1} is associated with Mn_3O_4; the peaks at 570 and 650 cm^{-1} are characteristic of Mn–O lattice vibrations [35].

3.6. Catalytic reactions

Table 2 gives conversion and selectivity results for the manganese oxide samples used as catalysts for the oxidation of 2-thiophenemethanol. All of the tested materials show

Table 2
Conversion and selectivity in the oxidation of 2-thiophenemethanol using the manganese oxide samples as the catalysts

	Conversion (%)	Selectivity (%)
Conventional OMS-2	19	100
2.45 GHz OMS-2	30	100
5.5 GHz OMS-2	50	100
Variable frequency OMS-2	40	100
OMS-2 precursor	89	100

100% selectivity to 2-thiophenecarboxaldehyde. The conventional OMS-2 shows the lowest conversion in the oxidation reaction. Cryptomelane prepared at the high microwave frequency (5.5 GHz) exhibits significantly higher conversion than that for the low-frequency OMS-2 (2.45 GHz). Conversion of 2-thiophenemethanol increases with increasing microwave frequency of hydrothermal treatment. The OMS-2 synthesized at VFMW operation (3–5.5 GHz) shows a conversion value between those for the high and low-frequency materials. The OMS-2 precursor reveals the highest 2-thiophenemethanol conversion, 89%. The catalyst was washed after the reactions with acetone and methanol, calcined, and reused for the same oxidation reaction. The conversion after the recycle was 72%.

4. Discussion

Synthesis times in the presence of microwave radiation, regardless of frequency, were 6 times less than those from conventional heating. The conclusion of the synthesis was determined, based on XRD analyses of the materials, on the presence of all of the characteristic intensities for OMS-2 in the XRD patterns. In addition, no broad precursor peaks were present in the sample patterns of OMS-2. Interaction of the microwaves with manganese oxide and water molecules that have high dielectric constants may be responsible for the accelerated synthesis.

All of the OMS-2 samples revealed fibrous morphologies. The OMS-2 precursor showed unidentified chunky particles. X-ray analyses showed that the precursor's pattern had one major peak associated with the Q-phase of cryptomelane at $d = 2.389$ Å; however, the other peaks were very broad. The material appears to be mainly amorphous, mixed-valent manganese oxide. TEM analysis revealed some order in parts of the OMS-2 precursor; namely, lattice fringes are visible among the disordered precursor material (see Fig. 3). OMS-2 synthesized at high microwave frequency (5.5 GHz) has a very different morphology than OMS-2 synthesized at low microwave frequency (2.45 GHz). OMS-2 synthesized at high microwave frequency is composed of both small fibers (<100 nm in length) and fibers of a size typical of OMS-2. The small crystallites are possible building blocks of the longer fibers. Microwave heating at a high frequency (5.5 GHz) may be responsible for formation of the smaller particles. The smaller particle size of the OMS-2 prepared at high microwave frequency (5.5 GHz) may be one reason for the higher catalytic activity of the material.

Raman spectroscopy data suggest that the precursor is a mixture of different manganese oxides. Fig. 12 illustrates the

spectra for synthetic cryptomelane and the precursor showing peaks in the range of 500–655 cm^{-1}. These bands can be attributed to mixed-valent Mn in the manganese oxide systems. The precursor sample showed different spectra in different areas, indicating that the precursor contains different manganese oxide species. One of the spectra for the precursor resembled the one for the synthetic OMS-2. This finding, in combination with XRD results, suggests that the precursor can be in an intermediate stage between a disordered manganese oxide and cryptomelane.

The precursor material showed remarkable conversion in the oxidation of 2-thiophenemethanol to 2-thiophenecarboxaldehyde. The precursor preserved its catalytic activity after recycling. The OMS-2 precursor has a very high BET surface area (273 cm^2/g) compared with the other manganese oxides. The precursor has a significant percentage of micropores (3.36%) and an average mesopore size of 64 Å. All of the other tested materials have significantly larger pore sizes (151–271 Å). The small size of the precursor micropores, along with the high surface area, might be responsible for the high catalytic activity. Small pores may better accommodate the ∼4 Å molecules of 2-thiophenemethanol and thus provide a suitable environment for their conversion.

The precursor shows a very different oxygen evolution profile than the OMS-2 samples. The precursor starts giving off oxygen at temperatures as low as 200 °C. All of the OMS-2 materials release oxygen at a relatively high temperatures (above 300 °C). The early release could supply the oxygen needed for the oxidation reaction. A high conversion (89%) is observed in the oxidation of 2-thiophenemethanol using the precursor as the catalyst. In addition, for the high-frequency OMS-2, oxygen evolution begins at around 315 °C, much earlier than for the other OMS-2 samples, resulting in superior catalytic activity. TGA of the materials confirmed the TPD results. Three major weight losses occur for all of the OMS-2 samples. The second weight loss, occurring at 450–650 °C, is consistent with the oxygen evolution from OMS-2 materials observed during TPD.

Application of microwave heating during the OMS-2 synthesis seems to have an effect on the catalytic activity. No significant differences in morphology, surface area, or thermal stability were observed between OMS-2 synthesized at different frequencies and that synthesized at a variable frequency. However, the material prepared in the presence of high-frequency microwave radiation (5.5 GHz) showed remarkable conversion in the oxidation reaction. Similar to the precursor, the high-frequency material showed a considerable percentage of micropores (2.00%), which could have enhanced its catalytic activity. Also, as in the case of the precursor, this could affect the suitability of the ∼4 Å 2-thiophenemethanol molecules in the pores. The smaller the pore size, the better the accommodation of the alcohol molecules and also the higher the conversion. Hydrothermal syntheses in the presence of higher-frequency microwave radiation (5.5 GHz) might result in an OMS-2 catalyst with improved activity for the oxidation of 2-thiophenemethanol to 2-thiophenecarboxaldehyde. Ru-supported materials as selective catalysts in the oxidation of 2-thiophenemethanol have been reported [36]. However, OMS-type materials would be a better alternative than a precious metal catalyst due to their much lower manufacturing costs.

The effect of variable frequencies acting on the manganese oxide precursor during the OMS-2 synthesis was not observed. The possible reason for this could be that small synthetic volumes (40 mL) were used, so that even single-frequency programs provided a sufficiently uniform electromagnetic field. Using a variable-frequency program may be beneficial for processing larger samples. In addition, the microwave ovens used in this research were a multimode type, which also gave good uniformity of the microwave field.

5. Conclusion

Our study of cryptomelane formation using microwave radiation heating has provided interesting information about its precursor. The disordered manganese oxide turned out to be a spectacular catalyst for the oxidation of 2-thiophenemethanol (conversion, 89%). Further studies will be conducted to evaluate its performance in other oxidation reactions. The mechanism of the oxidation reaction using the precursor as the catalyst will be also examined.

In addition, OMS-2 synthesized in the presence of microwave radiation revealed better conversions than obtained with conventionally prepared OMS-2. Hydrothermal treatment at a higher microwave frequency seems to be optimum for obtaining the most active cryptomelane for the oxidation of 2-thiophenemethanol.

Acknowledgments

The authors thank Dr. F.S. Galasso for helpful suggestions and discussions, Dr. K. Subramanian for the molecular size calculations, and NSF NIRT for funding (award CTS-0304217). The authors also thank the Geosciences and Biosciences Division, Office of Basic Energy Sciences, Office of Science, US Department of Energy for financial support.

References

[1] M. Abecassis-Wolfovich, R. Jothiramalingam, M.V. Landau, M. Herskowitz, B. Viswanathan, T.K. Varadarajan, Appl. Catal. B: Environ. 59 (1–2) (2005) 91.
[2] J. Liu, V. Makwana, J. Cai, S.L. Suib, M. Aindow, J. Phys. Chem. B 107 (35) (2003) 9185.
[3] S. Ching, E.J. Welch, S.M. Hughes, A.B.F. Bahadoor, S.L. Suib, Chem. Mater. 14 (3) (2002) 1292.
[4] R.N. De Guzman, Y.F. Shen, E.J. Neth, S.L. Suib, C.L. O'Young, S. Levine, J.M. Newman, Chem. Mater. 6 (1994) 815–821.
[5] J. Luo, Q. Zhang, A. Huang, S.L. Suib, Microporous Mesoporous Mater. (2000) 35–36, 209.
[6] X.F. Shen, J.S. Ding, J. Liu, J. Cai, K. Laubernds, R.P. Zerger, A. Vasiliev, M. Aindow, S.L. Suib, Adv. Mater. 17 (7) (2005) 805.
[7] J. Yuan, W. Li, S. Gomez, S.L. Suib, J. Am. Chem. Soc. 127 (41) (2005) 14184.
[8] X. Hong, G. Zhang, Y. Zhu, H. Yang, Mater. Res. Bull. 38 (13) (2003) 1695.
[9] S. Ching, J.L. Roark, Chem. Mater. 9 (1997) 750.

[10] J.C. Villegas, L.J. Garces, S. Gomez, J.P. Durand, S.L. Suib, Chem. Mater. 17 (7) (2005) 1910.
[11] J. Liu, Y.C. Son, J. Cai, X. Shen, S.L. Suib, M. Aindow, Chem. Mater. 16 (2004) 276.
[12] L. Valette, S. Poulain, X. Fernandez, L. Lizzani-Cuvelier, J. Sulfur Chem. 26 (2) (2005) 155.
[13] S.A. Mirji, Y.B. Khollam, S.B. Deshpande, H.S. Potdar, R.N. Bathe, S.R. Sainkar, S.K. Date, Mater. Lett. 58 (5) (2004) 837.
[14] D.A. Lewis, J.D. Summers, T.C. Ward, J.E. McGrath, J. Polym. Sci. A: Polym. Chem. 30 (8) (1992) 1647.
[15] M. Nüchter, B. Ondruschka, W. Lautenschlager, Synth. Commun. 31 (2001) 1277.
[16] E. Petricci, M. Botta, F. Corelli, C. Mugnaini, Tetrahedron Lett. 43 (37) (2002) 6507.
[17] G.D. Yadav, P.M. Bisht, Catal. Commun. 5 (5) (2004) 259.
[18] W.H. Sutton, Ceram. Bull. 68 (1989) 376.
[19] S. Barlow, S.R. Marder, Adv. Funct. Mater. 13 (2003) 7, 517.
[20] M. Tsuji, M. Hashimoto, Y. Nishizawa, M. Kubokawa, T. Tsuji, Chem. Eur. J. (2005) 11, 440.
[21] A. Fini, A. Breccia, Pure Appl. Chem. 71 (4) (1999) 573.
[22] M. Nüchter, et al., Chem. Eng. Technol. 26 (2003) 12.
[23] N.E. Leadbeater, Chem. Commun. 23 (2005) 2881.
[24] D.R. Baghurst, D.M.P. Mingos, J. Chem. Soc. Chem. Commun. 12 (1988) 829.
[25] D.R. Lide, CRC Handbook of Chemistry and Physics, 73rd ed., CRC Press, Boca Raton, FL, 1992, p. 12.
[26] D.M.P. Mingos, D.R. Baghurst, Brit. Ceram. Trans. J. 91 (1992) 124.
[27] H.S. Ku et al., Plast. Rubber Compos. 29 (2000) 6.
[28] C. Antonio, R.T. Deam, J. Mater. Process. Technol. 169 (2) (2005) 234.
[29] P.F. Mead, A. Ramamoorthy, S. Pal, J. Electronic Packaging 125 (2003) 295.
[30] D. Glover, B. Schumm, A. Kazowa, Handbook of Manganese Dioxides Battery Grade, Int. Battery Mater. Assoc., 1989.
[31] V.D. Makwana, et al., Catal. Today 85 (2003) 225.
[32] Y.G. Yin, W.Q. Xu, R.N. DeGuzman, S.L. Suib, C.L. O'Young, Inorg. Chem. 33 (1994) 4384.
[33] Y.G. Yin, W.Q. Xu, Y.F. Shen, S.L. Suib, C.L. O'Young, Chem. Mater. 6 (1994) 1803.
[34] Y.G. Yin, W.Q. Xu, S.L. Suib, C.L. O'Young, Inorg. Chem. 34 (1995) 4187.
[35] F. Buciuman, F. Patcas, R. Craciun, D. Zahn, Phys. Chem. Chem. Phys. 1 (1999) 185.
[36] K.G. Griffin, P. Johnston, S.C. Bennett, S. Kaliq, http://www.Chemicals.matthey.com.